Single-Molecule Spectroscopy Unmasks the Lowest Exciton State of the B850 Assembly in LH2 from *Rps. acidophila*

Ralf Kunz,[†] Kõu Timpmann,[‡] June Southall,[§] Richard J. Cogdell,[§] Arvi Freiberg,[‡¶] and Jürgen Köhler[†*]

[†]Experimental Physics IV and Bayreuth Institute for Macromolecular Research (BIMF), University of Bayreuth, Bayreuth, Germany; [‡]Institute of Physics, University of Tartu, Tartu, Estonia; [§]Institute of Molecular, Cell and Systems Biology, College of Medical Veterinary and Life Sciences, Biomedical Research Building, University of Glasgow, Glasgow, Scotland, United Kingdom; and [¶]Institute of Molecular and Cell Biology, University of Tartu, Tartu, Estonia

ABSTRACT We have recorded fluorescence-excitation and emission spectra from single LH2 complexes from *Rhodopseudomonas* (*Rps.*) *acidophila*. Both types of spectra show strong temporal spectral fluctuations that can be visualized as spectral diffusion plots. Comparison of the excitation and emission spectra reveals that for most of the complexes the lowest exciton transition is not observable in the excitation spectra due to the cutoff of the detection filter characteristics. However, from the spectral diffusion plots we have the full spectral and temporal information at hand and can select those complexes for which the excitation spectra are complete. Correlating the red most spectral feature of the excitation spectrum with the blue most spectral feature of the emission spectrum allows an unambiguous assignment of the lowest exciton state. Hence, application of fluorescence-excitation and emission spectroscopy on the same individual LH2 complex allows us to decipher spectral subtleties that are usually hidden in traditional ensemble spectroscopy.

INTRODUCTION

The initial event in bacterial photosynthesis is the absorption of a photon by a light-harvesting (LH) antenna system, which is followed by rapid and highly efficient transfer of the energy to the reaction center, where a charge separation takes place and the energy becomes available as chemical energy (1,2). In most purple bacteria, the photosynthetic membranes contain two types of LH complexes, the core RC-LH1 complex and the peripheral LH2 complex (3). The progress made in high-resolution structural studies of LH2 complexes of purple bacteria (4–6) has strongly stimulated theoretical (7–16) and experimental investigations on ensembles (17–25) as well as single molecules (26–36) to understand the efficient energy transfer in these antenna systems (3,23,37,38). The x-ray structure of the LH2 complex shows a remarkable symmetry in the arrangement of the light-absorbing pigments in their protein matrix. The basic building block of LH2 is a protein heterodimer ($\alpha\beta$), which accommodates three bacteriochlorophyll *a* (BChl *a*) pigments and one carotenoid molecule. These modules then oligomerize to produce the native circular or elliptical LH complexes. For LH2 from *Rhodopseudomonas* (*Rps.*) *acidophila* the LH2 complex consists of nine such $\alpha\beta$-polypeptide heterodimers. A striking feature of the organization of the 27 BChl *a* molecules is their separation into two parallel rings. One ring consists of a group of 18 closely packed BChl *a* molecules, with their bacteriochlorin planes parallel to the symmetry axis, absorbing at 850 nm (B850), whereas the other ring comprises nine well-separated BChl *a* molecules having their bacteriochlorin planes perpendicular to the symmetry axis of the complex, which absorb at 800 nm (B800) (4,6).

It has now been well established that the spatial arrangement of the pigments determines, to a large extent, the spectroscopic features of the complexes and that in these systems collective effects have to be considered to appropriately describe their electronically excited states (39). This leads to so-called Frenkel excitons, which arise from the interactions of the transition-dipole moments of the individual pigments corresponding to delocalized electronically excited states. Neglecting the slight dimerization of the B850 BChl *a* molecules, the proper eigenstates (exciton states) are characterized by a quantum number, k, which can take the values 0, ± 1, ± 2, ..., ± 8, 9. Because of the circular symmetry, only the states $k = \pm 1$ carry an appreciable transition-dipole moment, which makes them accessible for optical spectroscopy. Structural- and/or energetic heterogeneities are usually accounted for by random and/or correlated disorder in the site energies of the BChl *a* molecules (14,40–43). The main effects of disorder on the exciton manifold are, a mixing of the different exciton levels, a modification of the energy separation of the exciton levels and lifting their pairwise degeneracy, and a redistribution of oscillator strength to nearby states (3,23). Recent studies suggested that, even at room temperature, quantum coherence could play an important role for the energy transfer properties in these systems (44–49).

Although the exciton model appropriately describes the essential features registered in fluorescence-excitation and absorption spectroscopy of the LH complexes, there are several observations in the emission spectra that are inconsistent with this model. For example, in hole burning

Submitted December 16, 2013, and accepted for publication March 19, 2014.

*Correspondence: juergen.koehler@uni-bayreuth.de

Editor: Antoine van Oijen.

0006-3495/14/05/2008/9 $2.00

http://dx.doi.org/10.1016/j.bpj.2014.03.023

spectroscopy it was found that the lowest exciton state ($k = 0$) was distributed over a range of 120–140 cm^{-1} full width half-maximum (FWHM) (50–52) on the low energy side of the ensemble absorption spectrum, whereas the width of the respective ensemble emission spectrum exceeds this figure by more than a factor of two. Moreover, evidence has been found that the emission spectrum is essentially homogeneously broadened suggesting that exciton-phonon coupling for the transition from the relaxed excited state must be significant (52,53). This is in contrast to the quasiline absorption spectrum, which is mostly inhomogeneously broadened. To explain these conflicting observations a model has been put forward that involves exciton self-trapping in the B850 aggregate (52–54). Self-trapping of excitons is a well-known phenomenon in molecular crystals, and refers to the fact that due to exciton-phonon interaction, the exciton induces a structural reorganization of its environment, which lowers its energy to an extent that the excitation energy gets trapped on a limited region of the aggregate (55,56). In two previous works we have addressed this issue and found that the electron-phonon coupling strengths in the B850 excited state varies strongly as a function of time within an individual complex (57,58). A detailed analysis of the data yields that the fluctuating electron-phonon coupling strength in the B850 excited state manifold is one of the key mechanisms that cause the previously mentioned discrepancy between the excitation/absorption and emission spectra.

Another issue that has led to hot debates in the past was the discrepancy between hole burning and single-molecule experiments concerning the spectral position of the lowest exciton state, $k = 0$. If observable at all in single-molecule spectroscopy, the spectral position of the $k = 0$ transition was always very close to the $k = \pm 1$ bands (26,59), whereas the hole burning data suggested a spectral separation of ~200 cm^{-1} from these bands (50,51). Yet, the igniting idea of how to address these conflicting results was obtained in the previous study (58), where we elucidated the fluctuation of the electron-phonon coupling strength within an individual complex. These fluctuations manifest themselves as fluctuations of the emission spectrum with respect to both spectral position and spectral profile, thereby causing an experimental problem. Usually the recording of an excitation spectrum requires the use of optical band-pass filters in the detection path to suppress unwanted scattered light from the sample. As a consequence of the spectral fluctuations of the emission spectrum the overlap with the transmission range of the band-pass filters changes as a function of time. Here, we address these temporal spectral fluctuations in more detail by recording sequences of fluorescence-excitation and fluorescence-emission spectra from the same individual LH2 complex. Our study reveals that for ~65% of the LH2 complexes the $k = 0$ transition in the excitation spectra appears to be red-shifted to such an extent that it prevents the recording of the full spectrum due to spectral overlap with the transmission window of the detection filter. For the remaining LH2 complexes the comparison of the excitation and emission spectra allows for an unambiguous assignment of the lowest exciton state for which we find a spectral separation from the $k = \pm 1$ states of 209 cm^{-1}.

MATERIALS AND METHODS

Sample preparation

The isolation/purification process of LH2 complexes from the species *Rps. acidophila* (strain 10050) has been performed as previously described (60). Until use, a stock solution of the sample is stored in buffer solution (20 mM Tris/HCl, pH 8.0, 0.1% LDAO) in small aliquots at −80°C. For studying single complexes the concentration of the stock solution was diluted in several steps with the detergent buffer solution down to concentrations of ~10^{-11} M. The solution used for dilution in the last step contains 1.8% (w/w) polyvinyl alcohol (PVA; M_w = 30,000−70,000 g/mol; Sigma-Aldrich, St. Louis, MO). A drop of this solution was spin-coated onto a cleaned quartz (SiO_2) substrate for 10 s at 500 rpm and 60 s at 2500 rpm, resulting in amorphous polymer films with thicknesses of ~100 nm. The samples were immediately mounted in a liquid-helium cryostat and cooled to 1.2 K. For ensemble studies of LH2 complexes, the stock solution was diluted to concentrations of 10^{-6} M, and the same protocol has been followed as described previously.

Optical setup

All optical experiments have been performed using a homebuilt fluorescence microscope that can be operated in wide-field imaging mode or confocal mode. As light source, we used a continuous-wave tunable titanium-sapphire (Ti:Sa) laser (3900S, Spectra Physics, Santa Clara, CA) pumped by a frequency doubled continuous-wave neodymium-yttrium-vanadate (Nd:YVO_4) laser (Millennia Vs, Spectra Physics). Tuning the laser wavelength of the Ti:Sa in well-defined steps was achieved by rotating the intracavity birefringent filter with a motorized micrometer screw. Calibration of the laser frequency has been verified by a wavemeter (WaveMaster, Coherent, Santa Clara, CA) and the accuracy as well as the reproducibility was verified to be ~1 cm^{-1}.

Wide-field imaging

For wide-field imaging a 40 × 40 μm^2 region of the sample was excited around 855 nm through a band-pass (BP) excitation filter (either BP 858 nm/30 nm (center/width (FWHM)); Dr. Hugo Anders, Nabburg, Germany, or BP850/30; AHF Analysetechnik, AG, Tübingen, Germany). The emission from the sample was collected with a microscope objective (NA = 0.85; Mikrothek, Hamburg, Germany) that was mounted inside the cryostat, passed a set of band-pass filters (BP 900/50; AHF Analysetechnik), and was detected with a back-illuminated charge-coupled device (CCD) camera (TE/CCD-512-TKB; Roper Scientific or iKon-M 934 BR-DD; Andor Technology, Belfast, UK).

Fluorescence-excitation spectroscopy

For fluorescence-excitation spectroscopy on the individual complexes identified in the wide-field image the microscope was used in confocal mode (61). The fluorescence-excitation spectra have been recorded by continuously scanning the excitation wavelength with a rate of 3 nm/s (~50 cm^{-1}/s). To match the polarization of the incident radiation with the orientation of the transition-dipole moments of the absorption bands, the

linear polarization of the excitation light was changed by 6.4° by means of a half-waveplate between two successive laser scans. The signal passed a set of band-pass filters and was focused onto a single-photon counting avalanche photodiode (SPCM-AQR-16, Perkin-Elmer, Waltham, MA). As detection filters, two sets of band-pass filters have been used (BP1: 893/18; BP2: 900/48; Dr. Hugo Anders, AHF Analysetechnik). The excitation intensity was 100–150 W/cm^2, and the spectral resolution of the experiment was ~1 cm^{-1}.

Fluorescence-emission spectroscopy

For emission spectroscopy on individual complexes the sample was excited around 800 nm through a band-pass filter (BP 805/60; AHF Analysetechnik) with linearly polarized light. In order not to miss the narrow B800 absorptions the laser wavelength was wobbled over a range of 2–6 nm with a rate of 3 nm/s during data acquisition. The emitted signal passed a set of dielectric long-pass filters (LP830; AHF Analysetechnik), was spectrally dispersed in a spectrometer (SpectraPro-150, 300 or 600 lines/mm, Acton Research Corporation, Roper Scientific, Martinsried, Germany), and registered with a CCD camera. During the project we used three different CCD cameras (Luca-R 604M-OM/iDus DV420A-OE / iKon-M 934 BR-DD; Andor Technology), and depending on the type of camera used, the exposure times were 600 s/60 s/3–15 s, respectively. The spectral resolution varied as a function of the combination of grating and detector between 1.5 nm (20 cm^{-1}) and 0.5 nm (7 cm^{-1}). The excitation intensity was ~1 kW/cm^2.

RESULTS AND DISCUSSION

Fluorescence-excitation/emission spectroscopy on the same individual LH2 complex

The detection filters limit the possible scan range of the excitation laser from 770 to 876 nm for BP1 and from 770 nm to 872 nm for BP2. Because the peak position of the (ensemble) emission spectrum is at ~875 nm, and because the spectra from the individual LH2 complexes are heterogeneous, it is not clear a priori which scan range is sufficient (if at all) to obtain the entire excitation spectrum of the complex under study, or whether the excitation spectrum will be cut off at the red end. The influence of the detection filter on the resulting fluorescence-excitation spectrum from an individual LH2 complex is illustrated in Fig. 1, which shows data that have been recorded from three different individual LH2 complexes.

The left side, Fig. 1 *A*, refers to fluorescence-excitation spectroscopy, and the right side, Fig. 1 *B*, refers to emission spectroscopy on the same LH2 complexes. In Fig. 1 *A* the black lines correspond to the fluorescence-excitation spectra, and for comparison the gray lines indicate the emission spectrum obtained from the same complex. This color code is reversed in Fig. 1 *B*. We note that excitation and emission spectra cannot be measured simultaneously but have to be recorded subsequently. The colored areas in Fig. 1 *A* visualize the transmission ranges of the band-pass filters used in the detection path. For emission spectroscopy we used a set of long-pass filters that are transparent for light above 840 nm, as indicated by the green shaded area in Fig. 1 *B*, and excited the sample around 800 nm, where the excitation wavelength has been wobbled from 793 to 796 nm for complex I (800–803 nm for complex II; 791–797 nm for complex III), as shown by the blue shaded area in Fig. 1 *B*. We have verified that the exact spectral position of excitation in the B800 band had no influence on the emission spectrum. Because of the large spectral separation between excitation and detection, it is possible to record the full emission spectra from the individual LH2 complexes, as shown in Fig. 1 *B* by the black lines. Whether the fluorescence-excitation spectrum has been fully recorded or not can only be judged from comparison with the emission spectrum from the same complex. Only if the red edge of the excitation spectrum overlaps with the blue edge of the emission spectrum, the fluorescence-excitation spectrum

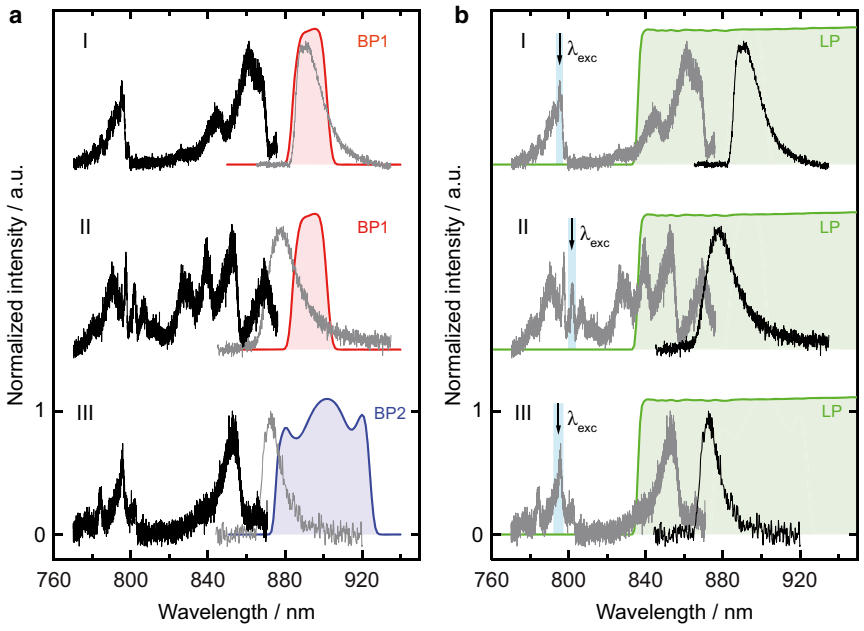

FIGURE 1 (*A*) Fluorescence-excitation spectra (*black lines*) from three individual LH2 complexes. The transmission characteristics of the detection filter used is shown by the colored areas. For comparison the corresponding emission spectra from the same complexes are indicated by the gray lines. (*B*) Emission spectra (*black lines*) from the same three individual LH2 complexes as in part (*A*). The transmission characteristics of the detection filter used is shown by the green area. The complexes are excited around 800 nm (*blue shaded area*) and the respective fluorescence-excitation spectra are shown by the gray lines for the ease of comparison.

can be considered as complete. Apparently, in Fig. 1 *A* this criterion is fulfilled for complexes II and III but not for complex I. Moreover, Fig. 1 *A* illustrates a possible conflict of interest for the experimentalist. To properly record the fluorescence-excitation spectrum the detection filter should only cut out the Stokes-shifted red tail of the emission spectrum (see complexes II and III, Fig. 1 *A*), whereas for obtaining the strongest signal the overlap between the transmission of the detection filter and the emission spectrum should be maximized (see complex I, Fig. 1 *A*). In other words, if the complexes would be selected from the wide-field image only, according to their signal strength, most fluorescence-excitation spectra would be as incomplete as for complex I shown in Fig. 1 *A* (see the Supporting Material).

The influence of spectral diffusion

Until now, we have treated all spectra as if they were stationary in time. However, the situation is much more complicated than this, because it is well known that both fluorescence-excitation and emission spectra show spectral diffusion. As an example, we show the fluorescence-excitation spectrum, Fig. 2 *A*, and the emission spectrum, Fig. 2 *B*, of complex II from Fig. 1 in a two-dimensional representation, which is commonly referred to as spectral diffusion plot.

For both patterns the horizontal axes correspond to wavelength, the vertical axes are equivalent to time, and the intensities are color coded. For the excitation spectra, Fig. 2 *A*, the vertical axis represents a stack of 65 (fluorescence-excitation) spectra recorded in rapid succession. The sum of these spectra is shown in Fig. 2 *C* by the black line (*top trace*). This is the same excitation spectrum as shown in Fig. 1 *A*, for complex II. For the emission spectra, Fig. 2 *B*, the vertical axis corresponds to 500 (*emission*) spectra that were consecutively recorded. The sum of the emission spectra is shown in Fig. 2 *C* by the gray line (*top trace*) and corresponds to the emission spectrum shown in Fig. 1 *B* for complex II. The spectral diffusion plot of the emission spectrum, Fig. 2 *B*, uncovers that for this complex the peak position of the emission spectrum can change by as much as 16 nm, which leads to a significant change of the spectral overlap between the emission spectrum and the transmission characteristics of the detection filter. Hence, during the recording of an excitation spectrum the emission might jump out of the detection window. This leads to periods of lower or even the absence of signal, as indicated by the arrow in Fig. 2 *A*, which might be misinterpreted as blinking, i.e., a reversible quenching of the fluorescence, although the fluorescence has not been quenched but has been spectrally shifted outside of the detection range.

Nevertheless, having the spectral diffusion plots at hand, we can search within the stacks of individual excitation/emission spectra for those where the reddest excitation and the most blue emission spectral bands coincide. For

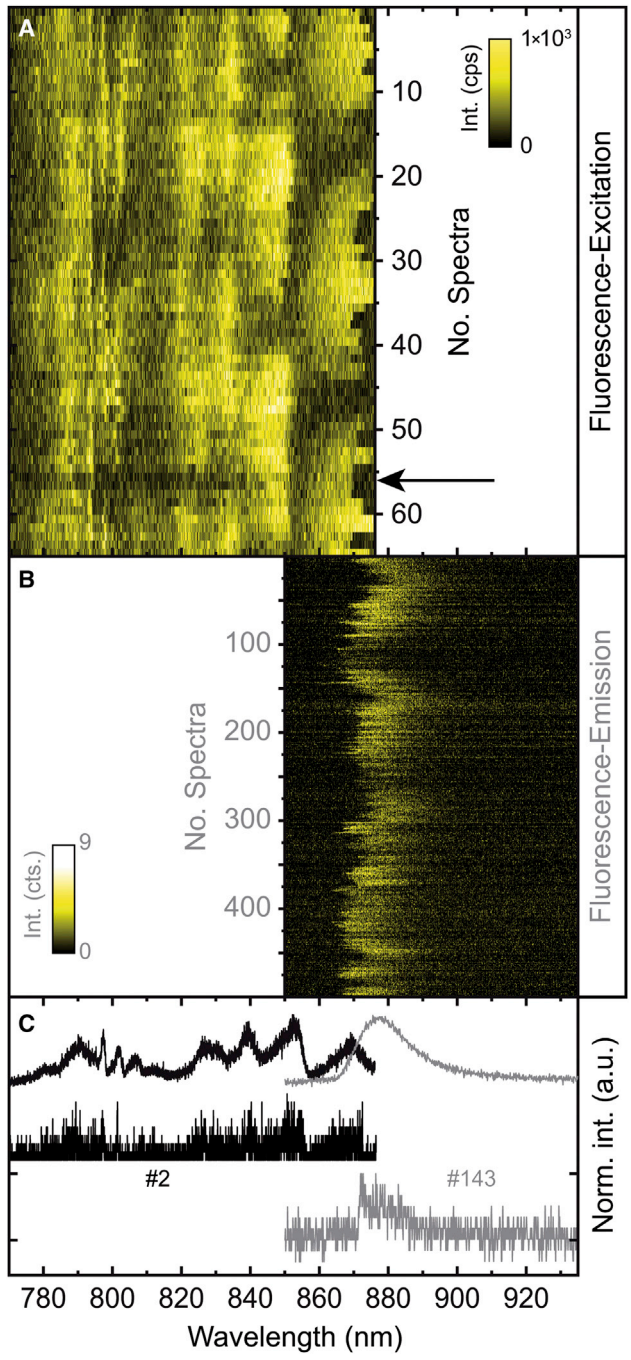

FIGURE 2 (*A*) Stack of 65 consecutively recorded fluorescence-excitation spectra from a single LH2 (complex II from Fig. 1). Between two successive scans the polarization of the incident radiation has been rotated by 6.4°. The duration for a single scan was 35 s, and the excitation intensity was 125 W/cm^2. The arrow denotes a time period with practically no signal as discussed in the text. (*B*) Stack of 500 consecutively recorded emission spectra from the same complex. The exposure time for an individual spectrum was 5 s. The excitation intensity was 1 kW/cm^2. (*C*) Top traces: Summed fluorescence-excitation spectrum (*black line*) and summed emission spectrum (*gray line*) from the corresponding stacks of spectra. Lower traces: Examples for a single fluorescence-excitation spectrum (*black line*) and a single emission spectrum (*gray line*) where the most red (*excitation*) and the most blue (*emission*) spectral bands overlap. All spectra have been peak normalized, and the individual spectra have been offset for clarity. To see this figure in color, go online.

the patterns displayed in Fig. 2, examples of such spectra are shown by the two lower traces in Fig. 2 *C*. Further examples from other individual LH2 complexes are shown in Fig. 3. For each part of this figure the top traces correspond to the summed excitation spectra (*black*) and to the summed emission spectra (*gray*) from a spectral diffusion plot (not shown), and the lower traces correspond to individual spectra that have been selected according to the previously mentioned coincidence requirement.

This selection procedure allowed us to extract complete fluorescence-excitation spectra from the spectral diffusion plots of 28 complexes (out of 74 complexes). From those spectra we determined the spectral peak positions of the absorption bands, and assigned these bands from red to blue to the $k = 0$, the $k = \pm 1$, and to higher exciton states, respectively. To check whether the restriction to those 28 complexes could lead to conclusions about the excitonic energy manifold that might not be representative for the ensemble of LH2 complexes, we compared the energetic separations between the spectral peak positions of the exciton states with those obtained in previous work (30,59,62–64), see Table 1.

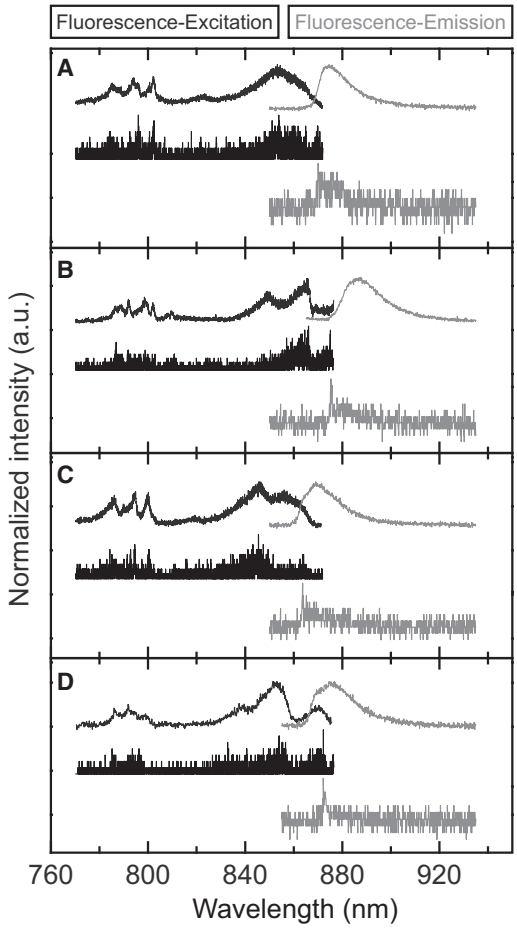

FIGURE 3 Examples of the summed (*top*) and individual (*bottom*) fluorescence-excitation spectra (*black*) and emission spectra (*gray*) from four individual LH2 complexes (*A–D*). The setup of each part of the figure is similar to the setup of Fig. 2 *C*.

In Table 1, ΔE_{01} denotes the mean energetic separation between the spectral position of the $k = 0$ state and the average spectral position of the $k = \pm 1$ states of an individual complex, $\Delta E_{\pm 1}$ denotes the energetic separations between the $k = \pm 1$ states of an individual complex, and for better comparison with previous work ΔE_{higher} denotes the energetic separation between the average spectral position of the $k = \pm 1$ states of an individual complex and the next higher exciton state of the same complex. The only significant discrepancy between the current study and previously obtained results concerns the energetic separation ΔE_{01}. However, this mismatch is simple to understand. First of all, to reduce the influence of spectral diffusion, the individual scans of the spectral diffusion plots in (59) have been shifted with respect to each other such that the spectral positions of the $k = 0$ transitions coincided. This step was crucial to make the $k = 0$ transitions visible, yet it scrambled all other parts of the spectrum and affects the information about the spectral separations between the exciton bands. But notwithstanding this problem it was possible for 3 of 19 complexes to observe the $k = 0$ transition and therefore to determine its spectral position. Based on our results here, we argue that the $k = 0$ transition for the remaining LH2 complexes might have been red-shifted to an extent that it overlapped with the detection window. Hence, complexes that featured a larger spectral separation between the $k = 0$ and $k = \pm 1$ exciton states did not contribute to the data evaluation. Yet, the energetic separation between the $k = \pm 1$ states, which is of crucial importance for modeling the energetic and geometric structure, is in close agreement for all studies and testifies that this parameter is not affected by having limited the LH2 complexes from which to select those with a full excitation spectrum.

To check whether the selection of the LH2 complexes according to the spectral position of the $k = 0$ state leads to a bias in the ΔE_{01} separation, we compared the spectral peak position of the red most band in the excitation spectra, and the peak position of the summed emission spectrum for the

TABLE 1 Energetic separation between the exciton states in the B850 manifold as obtained by single-molecule spectroscopy in different studies

Study	Number of complexes	ΔE_{01} (cm^{-1})	$\Delta E_{\pm 1}$ (cm^{-1})	ΔE_{higher} (cm^{-1})
Ketelaars (59)	19	84[a]	110	285
Hofmann (62)	144	–	126	–
Richter (30)	175	–	126[b]	–
Reichl (63)	19	238	129	272
Uchiyama (64)	89[c]/72[d]	–	90[c]/139[d]	–
this work	28	209	111	299

[a]In (59) $k = 0$ was detectable only for three of the 19 LH2 complexes.
[b]LH2 reconstituted into DOPC bilayer.
[c]LH2 reconstituted into DMPC bilayer.
[d]LH2 solubilized in OG micelle.

selected 28 individual complexes. The distribution of both parameters is shown in Fig. 4 *A* where we overlaid the ensemble fluorescence-excitation/emission spectra for comparison. The distribution of the spectral position of the most red band in fluorescence-excitation is centered at 11518 cm^{-1} ± 41 cm^{-1} (mean ± sdev); i.e., it is spectrally separated by ~170 cm^{-1} from the peak of the ensemble fluorescence-excitation spectrum. The distribution for the peak positions of the emission spectra is characterized by 11426 cm^{-1} ± 82 cm^{-1}. The width of this distribution corresponds to a FWHM of 194 cm^{-1}, which is about a factor of two larger than the width of the distribution for the most red absorption peak. This factor is in close agreement with what has been found for LH2 from *Rhodobacter sphaeroides* in buffer/glycerol solutions (52,65).

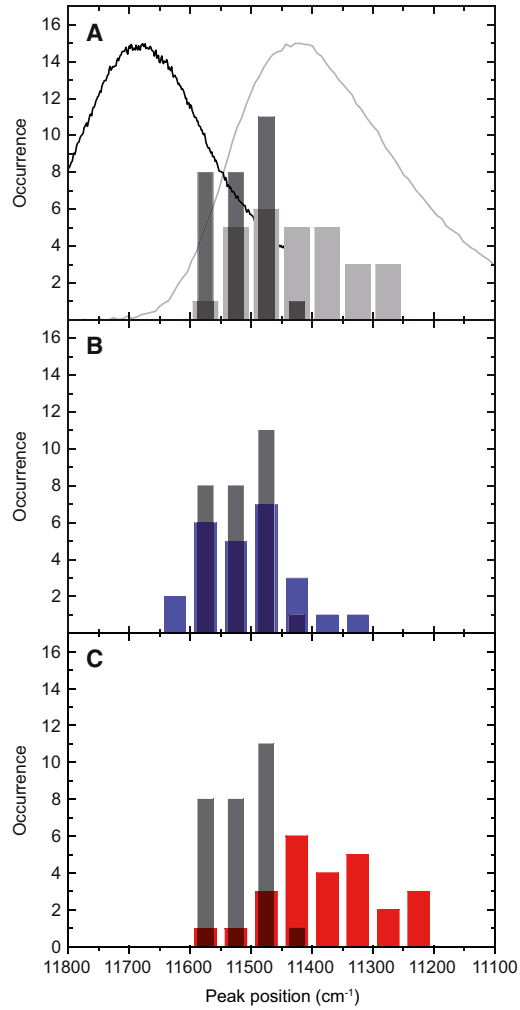

FIGURE 4 (*A*) Distribution of spectral peak positions of the most red excitation band in the excitation spectra (*black*) and distribution of the peak positions of the summed emission spectra (*gray*) for 28 LH2 complexes. For comparison the normalized fluorescence-excitation/emission spectrum (*black/gray line*) from a thin film of an ensemble of LH2 complexes has been overlaid. The distributions are characterized by 11518 cm^{-1} ± 41 cm^{-1} (mean ± sdev), and 11426 cm^{-1} ± 82 cm^{-1}, respectively. (*B*) Comparison of the distributions of the spectral peak positions of the most red excitation band (*black*) and the spectral peak positions of the most blue emission spectra (*blue*). The distribution of the latter is characterized by 11503 cm^{-1} ± 75 cm^{-1}. (*C*) Comparison of the distributions of the spectral peak positions of the most red excitation band (*black*) and the spectral peak positions of the most red emission spectra (*red*). The distribution of the latter is characterized by 11377 cm^{-1} ± 91 cm^{-1}. The histograms differ in the number of entries for the emission spectra (*A*): 28; (*B* and *C*): 25, because for three complexes only the time-averaged spectrum has been measured.

The observed spectral separation of 170 cm^{-1} between the mean of the distribution of the reddest band in absorption and the peak of the ensemble fluorescence excitation spectrum is in good agreement with the results from hole burning spectroscopy on ensembles of LH2 in buffer/glycerol solution. For LH2 from *Rb. sphaeroides* this separation amounted to (176 ± 10) cm^{-1} (66), and for LH2 from *Rps. acidophila* to 200 cm^{-1} (50); the width of the distribution of the zero-phonon hole action spectra for LH2 from *Rps. acidophila* was 120 cm^{-1}, compared to 97 cm^{-1} found here when the standard deviation of 41 cm^{-1} is converted to FWHM. Recently, however, the possibility of a static deformation of LH2 complexes due to the PVA matrix has been discussed in (36). To verify whether embedding the LH2 complexes in a PVA matrix deforms the structure of these antenna complexes and, therefore, introduces, per se, significant changes in their spectroscopic behavior, we reconstituted LH2 and RC-LH1 into a lipid bilayer and compared the spectra with those from complexes that were embedded in PVA (30,67). These studies revealed that at least for the LH complexes from purple bacteria, PVA is a good choice as a matrix that does not influence the conclusions drawn about the excitonic states in those pigment-protein complexes. In general, as any solvent it has an influence on the absolute spectral positions of the exciton bands. For example, at cryogenic temperatures the peaks of the ensemble spectra from the samples prepared in buffer/glycerol solution and PVA are shifted by ~189 cm^{-1} with respect to each other. More details about how the absolute spectral positions of the LH2 absorptions are influenced by the solvent and/or temperature can be found in (68,69).

As a matter of fact, both the fluorescence-excitation spectra and the emission spectra are affected by spectral diffusion, see for example Fig. 2. Although for each individual complex we dispose of the most blue/red emission spectra, and we can compare the spectral positions of those spectra with the distribution of the spectral positions that we assigned to the lowest exciton state ($k = 0$) in fluorescence excitation. These comparisons are shown in Fig. 4, *B* and *C*, respectively. Given the limited statistics both histograms in Fig. 4 *B* are in good agreement, which testifies that those histograms correspond to the distributions of the spectral positions of the zero-phonon lines (0–0 transitions) of the individual complexes. This is in clear contrast to the ensemble emission spectrum that deviates significantly from the mirror image of the ensemble absorption spectrum.

The reason for this deviation becomes clear when looking at Fig. 4 *C*, where we compare the spectral positions of the $k = 0$ state with the distribution of the most red emission spectra. Here, the mean of the distribution of the peak positions of the emission spectra is significantly red-shifted (by ~140 cm^{-1}) with respect to the mean of the distribution of the $k = 0$ state.

These finding are in line with previous work where we found that both spectral position as well as spectral profile of the emission spectrum of an individual complex undergoes strong fluctuations (58). Thereby, emission spectra featuring a distinctive zero-phonon line occurred predominantly at the blue end of the emission spectrum, whereas broad and featureless emission bands occurred preferentially at the red end of the emission spectrum, being again in good qualitative agreement with the data obtained on an ensemble of LH2 from *Rb. sphaeroides* in a buffer/glycerol solution (70). These spectral variations were ascribed to fluctuations of the electron-phonon coupling strength of an individual LH2 complex and to the formation of self-trapped exciton states. Because all these fluctuations are inherent to an ensemble of complexes these subtle details are averaged out in an ensemble emission spectrum, giving rise to the discrepancies between absorption and emission spectra mentioned in the Introduction.

Finally, we show in Fig. 5 the ensemble fluorescence-excitation and emission spectra that were reconstructed from our single complex spectra for an increasing degree of selectivity. Traces *A* in Fig. 5 show the fluorescence-excitation and emission spectra from a thin film of an ensemble of LH2 complexes. The next traces correspond to the sum spectra from all 74 individual LH2 complexes that have been investigated in this study, Fig. 5 *B*, and to the sum spectra restricted to those 28 complexes for which the entire fluorescence-excitation spectrum was obtained, Fig. 5 *C*. The latter excitation spectrum (*black line*) features a substructure at the red end, which is masked in the previous spectra. However, as we find out from analysis of the individual spectral diffusion plots, this substructure reflects not only the presence of the lowest exciton state, but it also contains contributions from (spectrally diffusing) higher exciton states blurring this substructure due to temporal averaging. If we manually refine the spectral diffusion plots from all individual fluorescence-excitation spectra where higher exciton bands affect the spectrum of the most red absorption band, we obtain the trace shown in Fig. 5 *D* (*black line*), which clearly reveals the substructure at the red end of the excitation spectrum due to the lowest exciton state and nicely overlaps with the shoulder in the corresponding summed emission spectrum (*gray line*). It is worth noting that the relative oscillator strength of the $k = 0$ transition cannot be obtained from Fig. 5 *D* by determining its relative contribution to the intensity of the whole B850 spectrum, because this spectrum has been constructed from selected data sets as explained in detail previously.

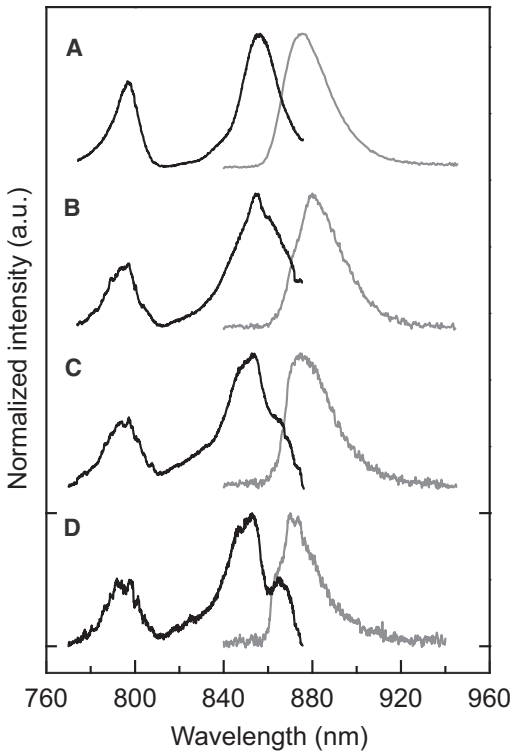

FIGURE 5 (*A*) Fluorescence-excitation (*black*) and emission (*gray*) spectra from an ensemble of LH2 complexes embedded in a PVA-film. (*B*) Summed fluorescence-excitation (*black*) and emission (*gray*) spectra from 74 LH2 complexes. For each complex the fluorescence-excitation/emission spectrum corresponds to the sum of all recorded individual scans/spectra for that complex as indicated in Fig. 2. (*C*) Summed fluorescence-excitation (*black*) and emission (*gray*) spectra from those 28 LH2 complexes for which an entire fluorescence-excitation spectrum has been recorded. For each complex the fluorescence-excitation/emission spectrum corresponds to the sum of all recorded individual scans/spectra for that complex as indicated in Fig. 2. (*D*) Summed fluorescence-excitation (*black*) and emission (*gray*) spectra from 21 (out of the previous 28) LH2 complexes. Here, for each complex only those individual fluorescence-excitation scans have been picked out from the spectral diffusion plots, for which no spectral overlap of the $k = 0$ and the higher exciton states occurred during the observation time due to spectral diffusion. For the summed emission spectrum only those emission spectra have been used, which showed an overlap with the $k = 0$ band in the corresponding fluorescence-excitation spectrum. Both types of spectra (fluorescence-excitation and emission) from each complex were first normalized and then summed up. All spectra are peak normalized and (*A–C*) have been offset for clarity. The data have been recorded at 1.2 K.

CONCLUSIONS

Having both fluorescence-excitation and emission spectra from the same individual LH2 complexes from *Rps. acidophila* at hand, shows that for ~2/3 of the complexes the fluorescence-excitation spectra are cut off at the red end due to overlap with the detection filter. However, selection of those LH2 complexes for which the fluorescence-excitation spectra were complete, together with the reduction of the influence of the spectral diffusion on the spectra by the sequential acquisition protocol, enabled us to locate the

spectral position of the lowest exciton state ($k = 0$) in their fluorescence-excitation spectra. The analysis of these data yields spectral separations between the $k = 0$ state and the higher exciton states that are in good agreement with the data obtained from hole-burning spectroscopy, solving an old puzzle that has been discussed in the community for more than a decade. Furthermore, we could shed light on the origin of the disagreement between the width of the distribution of the spectral position of the $k = 0$ state in absorption and the width of the ensemble emission spectrum.

SUPPORTING MATERIAL

One figure and supporting data are available at http://www.biophysj.org/biophysj/supplemental/S0006-3495(14)00323-3.

This work was financially supported by the Deutsche Forschungsgemeinschaft (KO 1359/16-1, GZ: 436 EST 113/4/0-1 and GRK1640) and the State of Bavaria within the initiative "Solar Technologies go Hybrid". K.T. and A.F. have been partially supported by the Estonian Research Council (IUT02-28). R.J.C. thanks the BBSRC for financial support.

REFERENCES

1. Blankenship, R. E., M. T. Madigan, and C. E. Bauer. 1995. Anoxygenic Photosynthetic Bacteria. Kluwer Academic Publishers, Dordrecht, The Netherlands.
2. Blankenship, R. E. 2002. Molecular Mechanisms of Photosynthesis. Blackwell Science, Oxford, United Kingdom.
3. Cogdell, R. J., A. Gall, and J. Köhler. 2006. The architecture and function of the light-harvesting apparatus of purple bacteria: from single molecules to in vivo membranes. *Q. Rev. Biophys.* 39:227–324.
4. McDermott, G., S. M. Prince, …, N. W. Isaacs. 1995. Crystal structure of an integral membrane light-harvesting complex from photosynthetic bacteria. *Nature.* 374:517–521.
5. Koepke, J., X. Hu, …, H. Michel. 1996. The crystal structure of the light-harvesting complex II (B800-850) from *Rhodospirillum molischianum*. *Structure*. 4:581–597.
6. Papiz, M. Z., S. M. Prince, …, N. W. Isaacs. 2003. The structure and thermal motion of the B800-850 LH2 complex from *Rps. acidophila* at 2.0 Å resolution and 100 K: new structural features and functionally relevant motions. *J. Mol. Biol.* 326:1523–1538.
7. Sauer, K., R. J. Cogdell, …, H. Scheer. 1996. Structure based calculations of the optical spectra of the LH2 bacteriochlorophyll-protein complex from *Rhodopseudomonas acidophila*. *Photochem. Photobiol.* 64:564–576.
8. Alden, R. G., E. Johnson, …, R. J. Cogdell. 1997. Calculations of spectroscopic properties of the LH2 bacteriochlorophyll-protein antenna complex from *Rhodopseudomonas acidophila*. *J. Phys. Chem. B.* 101:4667–4680.
9. Krueger, B. P., G. D. Scholes, and G. R. Fleming. 1998. Calculation of couplings and energy-transfer pathways between the pigments of LH2 by the ab initio transition density cube method. *J. Phys. Chem. B.* 102:5378–5386.
10. Mukai, K., S. Abe, and H. Sumi. 1999. Theory of rapid excitation energy transfer from B800 to optically forbidden exciton states of B850 in the antenna system LH2 of photosynthetic purple bacteria. *J. Phys. Chem. B.* 103:6096–6102.
11. Scholes, G. D., I. R. Gould, …, G. R. Fleming. 1999. Ab initio molecular orbital calculations of electronic couplings in the LH2 bacterial light-harvesting complex of *Rhodopseudomonas acidophila*. *J. Phys. Chem. B.* 103:2543–2553.
12. Mostovoy, M. V., and J. Knoester. 2000. Statistics of optical spectra from single ring aggregates and its application to LH2. *J. Phys. Chem. B.* 104:12355–12364.
13. Damjanović, A., I. Kosztin, …, K. Schulten. 2002. Excitons in a photosynthetic light-harvesting system: a combined molecular dynamics, quantum chemistry, and polaron model study. *Phys. Rev. E Stat. Nonlin. Soft Matter Phys.* 65:031919.
14. Jang, S., and R. J. Silbey. 2003. Single complex line shapes of the B850 band of LH2. *J. Chem. Phys.* 118:9324–9336.
15. Zhao, Y., M.-F. Ng, and G. Chen. 2004. Low-lying excited states of light-harvesting system II in purple bacteria. *Phys. Rev. E Stat. Nonlin. Soft Matter Phys.* 69:032902.
16. Ye, J., K. Sun, …, J. Cao. 2012. Excitonic energy transfer in light-harvesting complexes in purple bacteria. *J. Chem. Phys.* 136:245104.
17. Pullerits, T., and V. Sundström. 1996. Photosynthetic light-harvesting pigment-protein complexes: toward understanding how and why. *Acc. Chem. Res.* 29:381–389.
18. Monshouwer, R., M. Abrahamson, …, R. van Grondelle. 1997. Superradiance and exciton delocalization in bacterial photosynthetic light-harvesting systems. *J. Phys. Chem. B.* 101:7241–7248.
19. Freiberg, A., J. A. Jackson, …, N. W. Woodbury. 1998. Subpicosecond pump-supercontinuum probe spectroscopy of LH2 photosynthetic antenna proteins at low temperature. *J. Phys. Chem. A.* 102:4372–4380.
20. Freiberg, A., K. Timpmann, …, N. W. Woodbury. 1998. Exciton relaxation and transfer in the LH2 antenna network of photosynthetic bacteria. *J. Phys. Chem. B.* 102:10974–10982.
21. Sundström, V., T. Pullerits, and R. van Grondelle. 1999. Photosynthetic light-harvesting: reconciling dynamics and structure of purple bacterial LH2 reveals function of photosynthetic unit. *J. Phys. Chem. B.* 103:2327–2346.
22. Timpmann, K., N. W. Woodbury, and A. Freiberg. 2000. Unravelling exciton relaxation and energy transfer in LH2 photosynthetic antennas. *J. Phys. Chem. B.* 104:9769–9771.
23. Hu, X., T. Ritz, …, K. Schulten. 2002. Photosynthetic apparatus of purple bacteria. *Q. Rev. Biophys.* 35:1–62.
24. Timpmann, K., G. Trinkunas, …, A. Freiberg. 2004. Bandwidth of excitons in LH2 bacterial antenna chromoproteins. *Chem. Phys. Lett.* 398:384–388.
25. Timpmann, K., G. Trinkunas, …, A. Freiberg. 2005. Excitons in core LH1 antenna complexes of photosynthetic bacteria: evidence for strong resonant coupling and off-diagonal disorder. *Chem. Phys. Lett.* 414:359–363.
26. van Oijen, A. M., M. Ketelaars, …, J. Schmidt. 1999. Unraveling the electronic structure of individual photosynthetic pigment-protein complexes. *Science.* 285:400–402.
27. Bopp, M. A., A. Sytnik, …, R. M. Hochstrasser. 1999. The dynamics of structural deformations of immobilized single light-harvesting complexes. *Proc. Natl. Acad. Sci. USA.* 96:11271–11276.
28. Rutkauskas, D., J. Olsen, …, R. van Grondelle. 2006. Comparative study of spectral flexibilities of bacterial light-harvesting complexes: structural implications. *Biophys. J.* 90:2463–2474.
29. Berlin, Y., A. Burin, …, J. Köhler. 2007. Low temperature spectroscopy of proteins. Part II: Experiments with single protein complexes. *Phys. Life Rev.* 4:64–89.
30. Richter, M. F., J. Baier, …, S. Oellerich. 2007. Single-molecule spectroscopic characterization of light-harvesting 2 complexes reconstituted into model membranes. *Biophys. J.* 93:183–191.
31. Brotosudarmo, T. H. P., R. Kunz, …, J. Köhler. 2009. Single-molecule spectroscopy reveals that individual low-light LH2 complexes from *Rhodopseudomonas palustris* 2.1.6. have a heterogeneous polypeptide composition. *Biophys. J.* 97:1491–1500.
32. Oikawa, H., S. Fujiyoshi, …, M. Matsushita. 2008. How deep is the potential well confining a protein in a specific conformation? A single-molecule study on temperature dependence of conformational change between 5 and 18 K. *J. Am. Chem. Soc.* 130:4580–4581.

33. Tubasum, S., R. J. Cogdell, …, T. Pullerits. 2011. Excitation-emission polarization spectroscopy of single light harvesting complexes. *J. Phys. Chem. B.* 115:4963–4970.

34. Uchiyama, D., H. Oikawa, …, M. Matsushita. 2011. Reconstitution of bacterial photosynthetic unit in a lipid bilayer studied by single-molecule spectroscopy at 5 K. *Phys. Chem. Chem. Phys.* 13:11615–11619.

35. Rajapaksha, S. P., Y. He, and H. P. Lu. 2013. Combined topographic, spectroscopic, and model analyses of inhomogeneous energetic coupling of linear light harvesting complex II aggregates in native photosynthetic membranes. *Phys. Chem. Chem. Phys.* 15:5636–5647.

36. Tubasum, S., R. Camacho, …, I. G. Scheblykin. 2013. Evidence of excited state localization and static disorder in LH2 investigated by 2D-polarization single-molecule imaging at room temperature. *Phys. Chem. Chem. Phys.* 15:19862–19869.

37. Hu, X., A. Damjanović, …, K. Schulten. 1998. Architecture and mechanism of the light-harvesting apparatus of purple bacteria. *Proc. Natl. Acad. Sci. USA.* 95:5935–5941.

38. Robert, B., R. J. Cogdell, and R. J. van Grondelle. 2003. The light-harvesting system of purple bacteria. *In* Light-Harvesting Antennas in Photosynthesis. B. R. Green and W. W. Parson, editors. Kluwer Academic Publishers, Dordrecht, The Netherlands, pp. 169–194.

39. van Amerongen, H., L. Valkunas, and R. van Grondelle. 2000. Photosynthetic Excitons. World Scientific, Singapore.

40. Wu, H.-M., M. Rätsep, …, G. J. Small. 1997. Exciton level structure and energy disorder of the B850 ring of the LH2 antenna complex. *J. Phys. Chem. B.* 101:7654–7663.

41. Freiberg, A., K. Timpmann, …, N. W. Woodbury. 1999. Disordered exciton analysis of linear and nonlinear absorption spectra of antenna bacteriochlorophyll aggregates: LH2-only mutant chromatophores of *Rhodobacter sphaeroides* at 8 K under spectrally selective excitation. *J. Phys. Chem. B.* 103:10032–10041.

42. Jang, S., S. E. Dempster, and R. J. Silbey. 2001. Characterization of the static disorder in the B850 band of LH2. *J. Phys. Chem. B.* 105:6655–6665.

43. Matsushita, M., M. Ketelaars, …, J. Schmidt. 2001. Spectroscopy on the B850 band of individual light-harvesting 2 complexes of *Rhodopseudomonas acidophila*. II. Exciton states of an elliptically deformed ring aggregate. *Biophys. J.* 80:1604–1614.

44. Sumi, H. 2001. Bacterial photosynthesis begins with quantum-mechanical coherence. *Chem. Rec.* 1:480–493.

45. Harel, E., and G. S. Engel. 2012. Quantum coherence spectroscopy reveals complex dynamics in bacterial light-harvesting complex 2 (LH2). *Proc. Natl. Acad. Sci. USA.* 109:706–711.

46. Smyth, C., F. Fassioli, and G. D. Scholes. 2012. Measures and implications of electronic coherence in photosynthetic light-harvesting. *Philos. Trans. R. Soc. A.* 370:3728–3749.

47. Freiberg, A., M. Pajusalu, and M. Rätsep. 2013. Excitons in intact cells of photosynthetic bacteria. *J. Phys. Chem. B.* 117:11007–11014.

48. Strümpfer, J., M. Şener, and K. Schulten. 2012. How quantum coherence assists photosynthetic light-harvesting. *J. Phys. Chem. Lett.* 3:536–542.

49. Hildner, R., D. Brinks, …, N. F. van Hulst. 2013. Quantum coherent energy transfer over varying pathways in single light-harvesting complexes. *Science.* 340:1448–1451.

50. Wu, H.-M., N. R. S. Reddy, and G. J. Small. 1997. Direct observation and hole burning of the lowest exciton level (B870) of the LH2 antenna complex of *Rhodopseudomonas acidophila* (strain 10050). *J. Phys. Chem. B.* 101:651–656.

51. Wu, H.-M., M. Rätsep, …, G. J. Small. 1997. Comparison of the LH2 antenna complex of *Rhodopseudomonas acidophila* (strain 10050) and *Rhodobacter sphaeroides* by high pressure absorption, high pressure hole burning, and temperature dependent absorption spectroscopies. *J. Phys. Chem. B.* 101:7641–7653.

52. Timpmann, K., Z. Katiliene, …, A. Freiberg. 2001. Exciton self trapping in one-dimensional photosynthetic antennas. *J. Phys. Chem. B.* 105:12223–12225.

53. Freiberg, A., M. Rätsep, …, W. N. Woodbury. 2003. Self-trapped excitons in LH2 antenna complexes between 5 K and ambient temperature. *J. Phys. Chem. B.* 107:11510–11519.

54. Polivka, T., T. Pullerits, …, V. Sundström. 2000. Exciton relaxation and polaron formation in LH2 at low temperature. *J. Phys. Chem. B.* 104:1088–1096.

55. Rashba, E. I. 1982. Self-trapping of excitons. *In* Excitons. E. I. Rashba and M. D. Sturge, editors. North-Holland Publishing, The Netherlands, pp. 544–602.

56. Freiberg, A., and G. Trinkunas. 2009. Unravelling the hidden nature of antenna excitations. *In* Photosynthesis In Silico: Understanding Complexity from Molecules to Ecosystems. A. Laisk, L. Nedbal, and Govindjee., editors. Springer, The Netherlands, pp. 55–82.

57. Kunz, R., K. Timpmann, …, J. Köhler. 2012. Exciton self trapping in photosynthetic pigment-protein complexes studied by single-molecule spectroscopy. *J. Phys. Chem. B.* 116:11017–11023.

58. Kunz, R., K. Timpmann, …, J. Köhler. 2013. Fluctuations in the electron-phonon coupling of a single chromoprotein. *Angew. Chem. Int. Ed. Engl.* 52:8726–8730.

59. Ketelaars, M., A. M. van Oijen, …, T. J. Aartsma. 2001. Spectroscopy on the B850 band of individual light-harvesting 2 complexes of *Rhodopseudomonas acidophila*. I. Experiments and Monte Carlo simulations. *Biophys. J.* 80:1591–1603.

60. Cogdell, R., and A. M. Hawthornthwaite. 1993. Preparation, purification, and crystallization of purple bacteria antenna complexes. *In* The Photosynthetic Reaction Center. J. Deisenhofer and J. R. Norris, editors. Academic Press, San Diego, CA, pp. 23–42.

61. Lang, E., J. Baier, and J. Köhler. 2006. Epifluorescence, confocal and total internal reflection microscopy for single-molecule experiments: a quantitative comparison. *J. Microsc.* 222:118–123.

62. Hofmann, C., T. J. Aartsma, and J. Köhler. 2004. Energetic disorder and the B850-exciton states of individual light-harvesting 2 complexes from *Rhodopseudomonas acidophila*. *Chem. Phys. Lett.* 395:373–378.

63. Reichl, P. 2005. Spectroscopic investigation of the exciton states in the B850 band of LH complexes. Diploma Thesis, Universität Bayreuth, Bayreuth, Germany.

64. Uchiyama, D., H. Hoshino, …, T. Dewa. 2011. Single-protein study of photoresistance of pigment-protein complex in lipid bilayer. *Chem. Phys. Lett.* 511:135–137.

65. Freiberg, A., M. Rätsep, and K. Timpmann. 2012. A comparative spectroscopic and kinetic study of photoexcitations in detergent-isolated and membrane-embedded LH2 light-harvesting complexes. *Biochim. Biophys. Acta.* 1817:1471–1482.

66. Purchase, R., and S. Völker. 2009. Spectral hole burning: examples from photosynthesis. *Photosynth. Res.* 101:245–266.

67. Böhm, P. S., R. Kunz, …, J. Köhler. 2013. Does the reconstitution of RC-LH1 complexes from *Rhodopseudomonas acidophila* strain 10050 into a phospholipid bilayer yield the optimum environment for optical spectroscopy? *J. Phys. Chem. B.* 117:15004–15013.

68. Urboniene, V., O. Vrublevskaja, …, L. Valkunas. 2007. Solvation effect of bacteriochlorophyll excitons in light-harvesting complex LH2. *Biophys. J.* 93:2188–2198.

69. Kunz, R., K. Timpmann, …, A. Freiberg. 2013. Fluorescence-excitation and emission spectra from LH2 antenna complexes of *Rhodopseudomonas acidophila* as a function of the sample preparation conditions. *J. Phys. Chem. B.* 117:12020–12029.

70. Freiberg, A., M. Rätsep, …, G. Trinkunas. 2009. Excitonic polarons in quasi-one-dimensional LH1 and LH2 bacteriochlorophyll *a* antenna aggregates from photosynthetic bacteria: a wavelength-dependent selective spectroscopy study. *Chem. Phys.* 357:102–112.

Supporting Material for manuscript

Single-Molecule Spectroscopy Unmasks the Lowest Exciton State of the B850 Assembly in LH2 from *Rps. acidophila*

Ralf Kunz,[†] Kõu Timpmann,[‡] June Southall,[§] Richard J. Cogdell,[§] Arvi Freiberg,[‡ ¶] and Jürgen Köhler,[† *]

[†]*Experimental Physics IV and Bayreuth Institute for Macromolecular Research (BIMF), University of Bayreuth, 95440 Bayreuth, Germany*

[‡]*Institute of Physics, University of Tartu, Riia 142, Tartu EE-51014, Estonia*

[§]*Institute of Molecular, Cell and Systems Biology, College of Medical Veterinary and Life Sciences, Biomedical Research Building, University of Glasgow, Glasgow G12 8QQ, Scotland, UK*

[¶]*Institute of Molecular and Cell Biology, University of Tartu, Riia 23, Tartu EE-51010, Estonia*

* Correspondence: juergen.koehler@uni-bayreuth.de

SUPPORTING MATERIAL

1. Selection of a single complex for spectroscopy

Usually the selection of a single LH complex for spectroscopy takes place in two steps. First a 40 × 40 μm^2 region of the sample is excited around 855 nm with a laser and the red-shifted fluorescence from the individual complexes located in that area is registered with a CCD camera. Subsequently the optics is switched to the confocal mode such that the excitation volume coincides with one of the complexes observed with the CCD camera. The general problem that arises with this protocol is illustrated on the example of the ensemble fluorescence-excitation spectrum, Fig. S1 *A*, *B* black line, and the emission spectrum, Fig. S1 *A*, *B* grey line, of LH2 from *Rps. acidophila*. Emission from the Ti:Sa crystal in the infrared spectral region that propagates towards the detector is suppressed by an excitation filter, the transmission of which is shown by the black dashed line in Fig. S1 *A*, *B*. The fluorescence from the sample is detected through bandpass filter-sets, and the respective transmission curves are shown by the coloured areas in Fig. S1 *A*, *B*. The wide-field images from the same area of the sample that have been registered with the two different detection filters are shown in Fig. S1 *C*, *D*. At the bottom of the wide-field images the spotted LH2 complexes are shown schematically by the coloured dots, where the colour of each dot refers to a LH2 complex that has been identified with the corresponding detection filter. Owing to the better spectral coverage of the transmission characteristics of the blue detection filter with the emission spectrum from a LH2 ensemble, the number of complexes that can be identified is larger for this filter. Hence, the choice of the detection filter plays a crucial role for the selection of a single complex for spectroscopy, because some of the complexes might not be observable while others appear brighter/dimmer as a function of the detection filter.

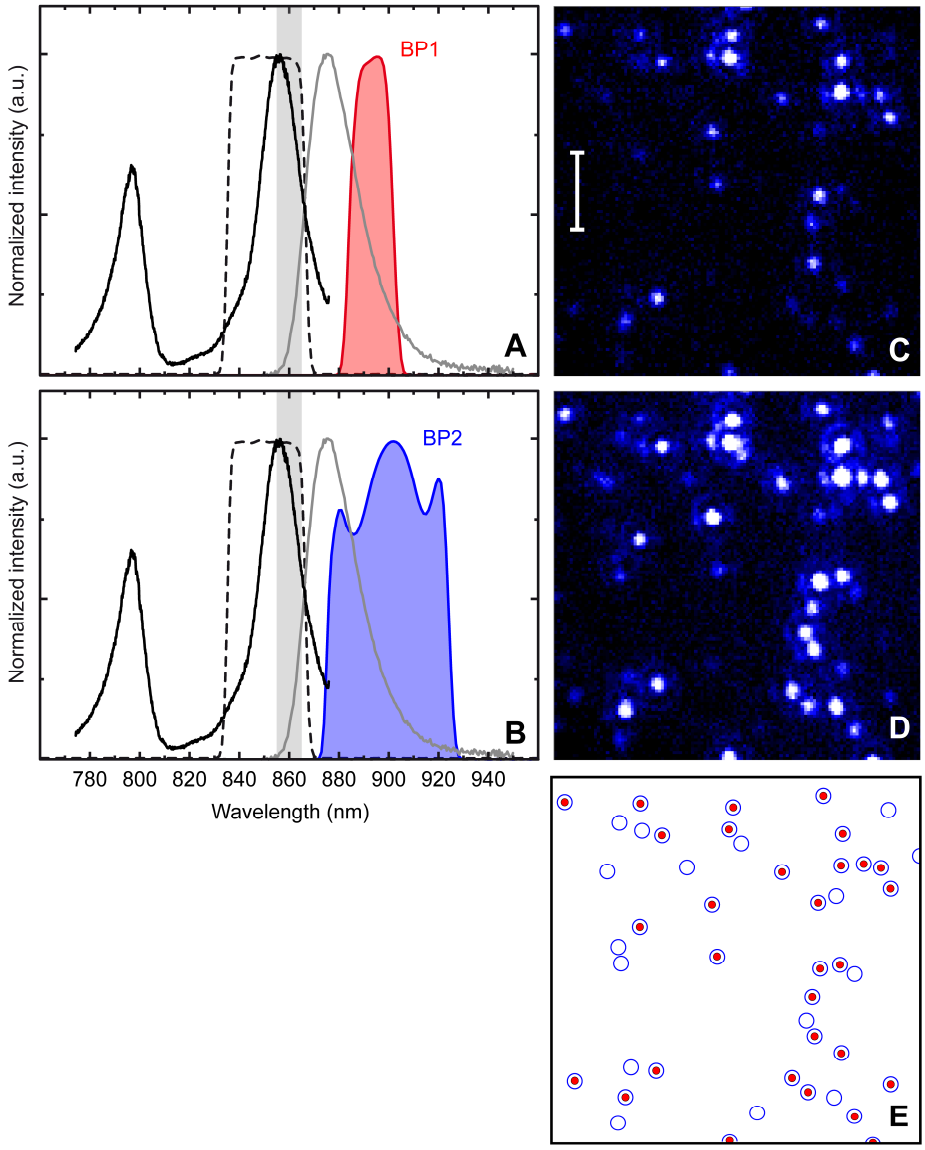

FIGURE S1 Left: Illustration of the influence of the spectral characteristics of the optical filters on the wide field imaging. Transmission curves of the detection filters with respect to the spectral positions of the absorption (*solid black lines*) and emission (*solid grey line*) of LH2 for two different detection filters. (*A*) BP1: center wavelength 893 nm, bandwidth 18 nm; (*B*) BP2: 900 nm, 48 nm. The *dashed line* corresponds to the transmission characteristics of a bandpass filter (850 nm, 30 nm) that is used in the excitation path to suppress background from the laser. All transmission curves of the optical filters are shown on a normalized scale. The sample is excited with circularly polarized light, the wavelength is wobbled between 855 nm and 865 nm (*grey shaded area*), and the excitation intensity is 100 W/cm^2. Right: Wide field images from the same sample area: (*C*) detected with filter BP1, (*D*) detected with filter BP2. The scale bar in (*C*) corresponds to 10 µm. (*E*) Schematic representation of the individual complexes that are identified in the two images. *Red dots* refer to part (*C*) of the figure (BP1), and *blue circles* refer to part (*D*) of the figure (BP2).